Proceedings of the 2005 IEEE
International Conference on Mechatronics
July 10-12, 2005, Taipei, Taiwan

# Fiber Image Techniques in Digital Stereomicroscopy

Kuang-Chao Fan[1, 2], Ruijun Li [1], Hsin-Ming Song [2], Koung-Ming Yeh[3]
[1]School of Instrumentation, Hefei University of Technology, Anhui China
[2]Department of Mechanical Engineering National Taiwan University, Taipei, Taiwan
[3]Metal Industries Research Development Centre, Kaohsiung, Taiwan
e-mail: fan@ntu.edu.tw

**Abstract**

**On the basis of the principle of structured light and phase shifting, a novel digital stereomicroscopes system for micro-3D inspection is presented in this paper. Because the image fiber has many advantages like direction changing and long distance transmitting without extra optics, this system also adopts it to project the structured light instead of the pure optical systems. Thus, the measurement head is very small, the measurement distance and orientation could be changed expediently. Experiments showed this is a useful system to measure the 3D profile of meso- to micro-scaled parts, such as the MEMS product.**

**Keywords: Micro 3D profile, Fiber image, Stereomicroscopy.**

## 1. INTRODUCTION

The microscope has been a widely used tool for 2-D visual inspection in science, industry and medicine. For many applications, however, the 2-D inspection is no longer sufficient to meet the need. The determination of three-dimensional (3-D) topography of the specimen is a task that is becoming more and more important.

Recently, many different measuring setups of stereomicroscopy based on structured light projection and triangulation principle for 3-D topographic measurements have been carried out. Windecker et al [1] and Wu [2] used physical gratings and the phase shift mechanism to project the structured light patterns onto the object surface, and then captured the deformed pattern with a CCD camera. Zhang et al [3] created computer generated patterns and its phase shifts, and then projected the patterns onto the surface through a commercial digital light processing (DLP). Their measurement results are all satisfactory. But, most of them are modified from the conventional visual stereomicroscopes. There are some drawbacks in this kind of system: (1) the specimen has to be preprocessed and fixed on the sample stage, (2) the stereoscopic angle is limited to the range of 10 to 20 degrees between the project axis and the viewing axis depending on the stereomicroscope in use, and (3) the field of view (FOV) is limited by the microscope's objective lens. Song [4] developed an independent stereomicroscope system composed of a PC to generate fringe patterns and to analyze the deformed patterns, a DLP to project the patterns, an optical lens system to guide the light, a stand to mount the lens, a XY stage to place the sample, and a zooming CCD camera to capture the image, as shown in Fig. 1. Because of the adjustable angle of the CCD and the selectable lens system, the above-mentioned drawbacks (2) and (3) can be overcome. However, if the scope head (or called the probe head) can be freely moved, the system would be more flexible to fit the object position, and can even to measure a selected portion of a large object.

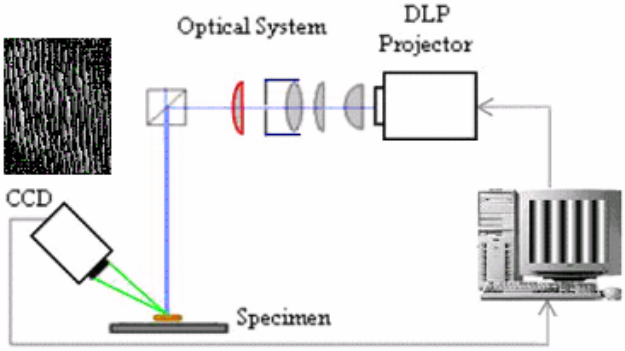


Fig. 1: Schematic diagram of the digital structured light stereomicroscope [4].

In this paper, we present a new stereomicroscopy configuration utilizing an image fiber bundle to direct the projecting patterns to any required angle via a developed miniature probe head. This is based on the concept of "instrument fits the objects" rather than "sample pieces fit the instrument". This setup not only extends the range of possible applications enormously, but also makes the measurement more flexible. The principle and the setup of our digital stereomicroscopes are introduced in Section 2; two important subsystems are discussed in this part. Section 3 details the optical design of the telecentric lens. Section 4 analyzes the characteristics of image fiber in detail. Some experimental results are presented in Section 5, and conclusions are given in Section 6.

## 2. STEREOMICROSCOPY BY STRUCTURED LIGHT PROJECTION

### *2.1 System configuration*

One method of 3D profile measurement techniques is to project the specially designed structured light pattern onto

the object's surface. The pattern can be of any structure, such as the light-dot-array, periodical sine waves, concentric circle, or 2D codes, etc. Due to the variation of the object's surface profile, the structured pattern will be deformed on the surface. A CCD camera can capture the deformed image. The object's three-dimensional contour data can be analyzed based on the principle of triangulation and phase shifting techniques. This process is also called "Reverse Engineering". If the object to be measured is very small in size, the light pattern should be reduced its projecting area by lens system, and the tiny image should be captured by the CCD via a zoom lens. This is a kind of stereomicroscope system as given in Fig. 1 [4]. However, the specimen has to adapt to the instrument.

A new stereomicroscopy configuration utilizing an image fiber bundle to direct the projecting patterns to any required angle via a developed miniature probe head is proposed to combine the fringe patterns projection technique with the specially designed optical system and the probe head. The system schematic diagram is depicted in Figure 2. The PC can generate black and white periodical sine patterns. Projected out through the DLP the patterns are entered into the image fiber bundle through a directly coupled telecentric optical system. The single mode image fiber bundle can then transmit the patterns to its output end and project onto the specimen through an objective lens system. The line pitch and the intensity can be adjusted by software according to the surface properties of the specimen. The fringes will be distorted by the topography of the specimen, and a CCD camera can capture this distorted image. Phase shifting technique is also applied for 3D reconstruction to better resolution.

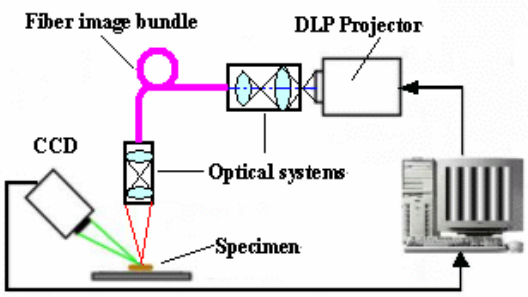


Fig. 2: Schematic diagram of fiber image transmitted stereomicroscope

The DLP used is directly purchased from the market. This new fringe projection system can easily produce fringe patterns with high brightness, contrast, and spatial accuracy, which is critical in achieving high resolution and accuracy in 3-D surface contouring. Although it is built up with a complicate DMD (Digital Micro-mirror Device) technology, its operation principle can be found in many references [5, 6]. This report does not describe its details. Followings will focus on the phase shifting principle, optical system design, and image fiber technique in sequence.

*2.2 Phase shifting technique*

Phase shifting technique is also a well-known method used for 3D reconstruction in reverse engineering or interferometry [7,8]. For the completeness of this report we shall give a simple expression.

Since the triangulation method only solve the surface heights corresponding to the pattern line centers. In order to increase the measurement resolution, any point between two adjacent lines we have to know its corresponding phase so as to convert its relative proportional height. Phase shifting of sinusoidal pattern is an effective solution. This research adopts four phase shifts method.

Let the image intensity of any pixel on the image frame be expressed by

$$I(x,y) = I_0(x,y)\cdot\{1+\gamma(x,y)\cdot\cos[\phi(x,y)]\} \quad (1)$$

where, $(x,y)$ represents the pixel coordinate, $I(x,y)$ is its corresponding image intensity, $I_0(x,y)$ is the constant background intensity, $\gamma(x,y)$ indicates the modulated amplitude of the sinusoidal pattern light at this pixel point, and $\phi(x,y)$ is the corresponding phase. There are three unknowns in Eq. (1), namely, $I_0(x,y)$, $\gamma(x,y)$, $\phi(x,y)$. Therefore, we need at least three equations to solve these unknowns simultaneously. The intensity of any pixel point at each phase shift can be expressed by

$$\begin{aligned} I_1(x,y) &= I_0(x,y)\cdot\{1+\gamma(x,y)\cdot\cos[\phi(x,y)]\} \\ I_2(x,y) &= I_0(x,y)\cdot\{1+\gamma(x,y)\cdot\cos[\phi(x,y)+\pi/2]\} \\ I_3(x,y) &= I_0(x,y)\cdot\{1+\gamma(x,y)\cdot\cos[\phi(x,y)+\pi]\} \\ I_4(x,y) &= I_0(x,y)\cdot\{1+\gamma(x,y)\cdot\cos[\phi(x,y)+3\pi/2]\} \end{aligned} \quad (2 \text{ to } 5)$$

Solving equations 2 to 5 we can obtain the phase of each point.

$$\phi = \tan^{-1}\left[\frac{I_4 - I_2}{I_1 - I_3}\right] \quad (6)$$

Eq. (6) only provides the phase of the said pixel point corresponding to its left and right adjacent pattern lines which contain only one cycle of the sinusoidal pattern. To connect discontinuous phases into continuous phases within a whole picture frame, the phase unwrapping process is needed [9, 10]. The rule is to accumulate the phase intervals step by step.

*2.3 Triangulation method*

As shown in Fig. 3, the geometrical relationship among structured light emitting point *P*, the CCD lens center *l*, and the point of projection on the object surface D forms up a triangulation. Without the object the DMD center shall project onto the reference plane at point *O*, and any point of the pattern shall project onto the reference plane at an offset position, say point *A*. Due to the surface height *BD*, point *A* will shift to point *C* on the image plane. The difference in phases of point A and C on the image plane can be expressed by $\phi_{AC} = \phi_C - \phi_A$. From the triangulation principle we can obtain the following equation. Distances *l* and *d* are

known during the system setup. The constant $K$ can be obtained by the calibration of gauge blocks.

$$\overline{DB} = \frac{l}{d}\overline{AC} = K\phi_{AC} = K(\phi_C - \phi_A) \tag{7}$$

*2.4 Optical system design*

Three optical modules are employed in this system; two at both ends of the image fiber bundle and the third one is equipped to the CCD camera. In order to enhance the measurement precision, all optical modules are designed by telecentricity [11].

Telecentricity is a special property of certain multi-element lens designs in which the chief rays for all points across the

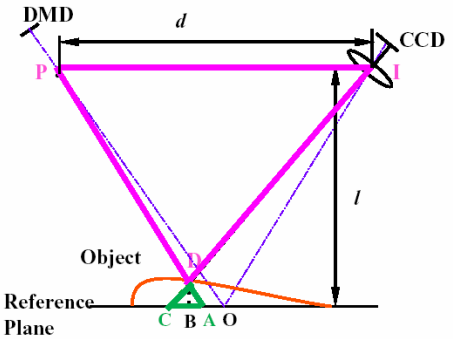


Fig. 3: Triangulation principle

object or image are collimated and are parallel to the optical axis. Telecentricity is desirable because it provides nearly constant magnification over a range of working distances, virtually eliminating perspective angle error. They can lead to extremely uniform image plane illumination. This means that object movement does not affect image magnification. For a system with object space telecentricity, movement of the object toward or away from the lens will not result in the image getting bigger or smaller, and an object which has depth or extent along the optical axis will not appear as if it is tilted. If not telecentricity, this type of instrument would give a different measurement result each time the working distance to the object was changed. All the optical systems in our system, therefore, are both object space and image space telecentricity. There are at least three benefits we do like this:

(1) Since the deviation of the object or image plane in a certain range will not change the image size for telecentricity. So, the distances between DLP and the zoom optical system, and between zoom optical system and the input end of the image fiber bundle, do not need to be very accurate. Therefore, the assembly of our system becomes more convenient.

(2) The object to be measured has depth change along the optical axis, so it is easy to project and capture the clear fringe patterns from the bottom to the top of the object by telecentricity. However the depth of field of non-telecentric lens is very little.

(3) Clear and uniform images, which contribute to the following works, such as image processing, edge detection, 3D reconstruction and so on, can be obtained by telecentricity. Because only the lights that parallel the optical axis can pass it.

For the clarity of expression, we assign the optical system connecting the DLP output and the fiber image bundle input as Optical System 1; the one between the fiber output and the object as Optical System 2; and the one between the object and the CCD input as Optical System 3. The design of each optical system is described as follows.

Optical system normally considers two stages. The first stage is the dimensional design to determine the field of view (FOV), focusing range, lens diameter, and the numeric aperture (NA). The second stage is the system aberration design, such as the lens type and the lens material, etc. The second stage can be assisted by a CAD tool, such as the ZEMAX.

Fig. 4 shows the configuration of one optical system. Let the focal lengths of the object and the image be $f_1$ and $f_2$ respectively; object size and image size be $y_1$ and $y_2$ respectively; the distance from the object to the focal point of objective lens be $x_1$; and the distance from the image to the focal point of the image's objective lens be $x_2$. The pin hole diameter is d, the tilted angles at both sides of the pin hole are $u_1$ and $u_2$, respectively. The diameter of the objective lens at the object side is $D_1$, and at the image side is $D_2$. The depth of focus of the objective lens at the object side is $\Delta_1$, and at the image side is $\Delta_2$.

From the Newton's Law we have:

$$\frac{f_1}{f_2} = \frac{y_1}{y_2} \tag{8}$$

$$\frac{x_2}{x_1} = \frac{f_2^2}{f_1^2} \tag{9}$$

Since $y_1$ and $y_2$ are known, the values of $f_1$, $f_2$, $x_1$, $x_2$ can be determined by equations (8) and (9).

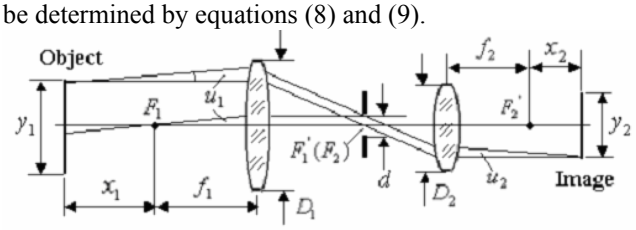


Fig. 4: Configuration of one Optical System

Any point of the object will form the radius of confusion disc ($R$) on the image plane. This radius $R$ is composed of three sources: the radius of Airy disc ($R_1$), the radius of the confusion disc due to the offset from the ideal image plane ($R_2$), and the radius of confusion disc due to the system aberration ($R_3$). The magnitude of $R$ is the convolution of $R_1$, $R_2$, and $R_3$, among which

$$R_1 = \frac{0.61 \cdot \lambda}{n_2 \cdot \sin u_2} \qquad R_2 = \frac{\Delta_2}{2} \cdot \tan u_2$$

Suppose that the resolution of the CCD (pixel space) is $c$. In

order to match the optical resolution to the CCD resolution, considering that after CCD calibration the $R_3$ can be negligible, we can let $R1 + R2 = c$ .

$$\frac{0.61 \cdot \lambda}{n_2 \cdot \sin u_2} + \frac{\Delta_2}{2} \cdot \tan u_2 = c \tag{10}$$

Since the angle of $u_2$ is small, we can assume $\sin u_2 \approx \tan u_2$. We can solve $\sin u_2$ from Eq. (10), and then solve the Numerical Aperture from NA'= $n_2 \sin u_2$. Moreover, according to the Lach invariant formula: $y_1 f_1 \tan u_1 = -y_2 f_2 \tan u_2$, we can find the NA of the objective lens from NA= $n_1 \sin u_1 \approx \tan u_1$.. Consequently, we can find $d$, $D_1$, and $D_2$ from the following equations:

$$d = 2 f_1 \cdot \tan u_1 = 2 f_2 \cdot \tan u_2$$
$$D_1 = y_1 + 2 f_1 \cdot \tan u_1$$
$$D_2 = y_2 + 2 f_2 \cdot \tan u_2$$

Once all parameters of $f_1$, $f_2$, $x_1$, $x_2$, $d$, $D_1$, $D_2$, $NA$ and $NA'$ are determined, we can process the optimum light trace with ZEMAX software.

According to the above analysis, Table 1 to Table 3 summarize the relevant parameters of optical systems 1 to 3. Fig. 5 shows the light tracing plot of Optical System 2. Fig. 6 shows the image distortion curve of Optical System 2 by the ZEMAX analysis. It is seen that the maximum distortion is below 0.5% and the diameter of dispersion disc at the marginal point of the field of view (FOV) is less than $10\,\mu m$ .

Table 1: Parameters of Optical System 1 (unit: mm)

| Focal length (object/image) | N.A. (object/image) | Resolution (LP/mm) (object/image) |
|---|---|---|
| 54.4/13.2 | 0.015/0.06 | 120/120 |

| Object FOV | Image FOV | $x_1 + f_1$ | $x_2 + f_2$ |
|---|---|---|---|
| $\phi 25$ | $\phi 6$ | 75 | 18 |

Table 2: Parameters of Optical System 2 (unit: mm)

| Focal length (object/image) | N.A. (object/image) | Resolution (LP/mm) (object/image) |
|---|---|---|
| 36.9/12.8 | 0.06/0.04 | 120/120 |

| Object FOV | Image FOV | $x_1 + f_1$ | $x_2 + f_2$ |
|---|---|---|---|
| $\phi 6$ | $\phi 8$ | 18 | 25 |

Table3: Parameters of Optical System 3 (unit: mm)

| Focal length (object/image) | N.A. (object/image) | Resolution (LP/mm) (object/image) |
|---|---|---|
| 17.6/13.2 | 0.04/0.06 | 120/120 |

| Object FOV | Image FOV | $x_1 + f_1$ | $x_2 + f_2$ |
|---|---|---|---|
| $\phi 8$ | $\phi 6$ | 56 | 17 |

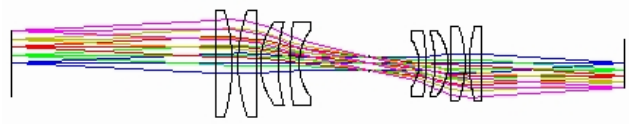

Fig. 5: Light tracing diagram of Optical system 2.

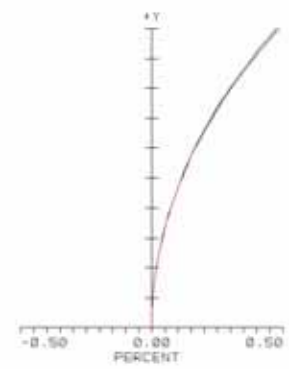


Fig. 6: Image distortion curve of Optical System 2.

## 3. IMAGE FIBER TECHNIQUES

### *3.1 Principle and characters of image fiber*

Single optical fiber consists of a core with higher refractive index and the coating with lower refractive index. It can transmit optical signal from its input end to the output end when the incidence angle of the optical ray is greater than the critical angle of the optical fiber. Single fiber can only transmit one dot signal.

Image fiber bundle is made up of thousands of single optical fibers, which are arrayed together by the coherent regulation of hexagon or square. The certain single optical fiber's position in input cross-section of image fiber is corresponding to its position in the output cross-section strictly. Hence, image fiber bundle can transmit picture from its input end to the output end clearly, and every single optical fiber in image fiber is just like a pixel in CCD array, as shown in Figure 7.

Fig. 7: The principle of image fiber

Compared with ordinary optical system, image fiber has many advantages when transmitting image, such as: (1) it can transmit image in certain bended state; (2) it is easy to acquire longer working distance; (3) it is smaller in volume and lighter in weight; (4) it has immunity to interference; (5) its structure is simple, etc. Because of these good properties, image fiber has been widely used in many fields, such as medical endoscopes [12], weapons, industry and so on.

Many factors of image fiber will affect the quality of the transmitted image, among which its numerical aperture (NA), attenuation, resolution and the image elements are the most important indices [13]. How to affect and how to choose image fiber properly will be addressed as follows:

(1) Numerical aperture (NA) is a basic optical characteristic of an image fiber. It is a measure of the acceptance angle of a single fiber. It can be thought of as representing the size or "degree of openness" of the input acceptance cone in Fig. 8. Mathematically, numerical aperture is defined as the sine of

the half-angle of the acceptance cone ($\sin A$).

$$NA = n_0 \cdot Sin(A_{\max}) = \sqrt{n_1^{\,2} - n_2^{\,2}} \qquad (11)$$

In this equation $A_{\max}$ is the half-angle or the critical angle within which light will be accepted and conducted through a fiber, $n_0$ is the refractive index outside the fiber end (air =1.0), $n_1$ is the refractive index of the core, and $n_2$ is the refractive index of the clad.

The light-gathering power or flux-carrying capacity of a fiber is proportional to the square of the numerical aperture. This is the ratio between the area of a unit sphere within the acceptance cone and the area of a hemisphere. A fiber with a numerical aperture of 0.66 has 43 percent of the flux-carrying capacity of a fiber with a numerical aperture of 1.0. So, the higher numerical aperture is, the more lights are gathered into the fibers, and the brighter images will be produced. In addition, higher numerical aperture means higher resolution.

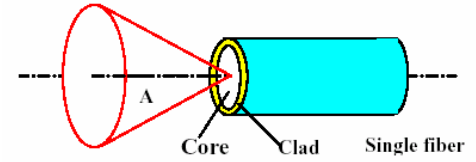


Fig. 8: The illumination of numerical aperture

(2) Attenuation means the intensity of the light decreases as it moves along the fiber. It can be specified in *db. Km*$^{-1}$, and calculated by the following formula:

$$Attenuation = 10\log_{10}\left(\frac{I_{out}}{I_{in}}\right) \qquad (12)$$

where, $I_{out}$ is the outgoing intensity (intensity is measured in W.m$^{-2}$) and $I_{in}$ is the ingoing intensity.

(3) Resolution can be defined as the ability of an image fiber to allow one to distinguish among small objects. The definition of the transmitted image is usually decided by the resolution of image fiber. The main factors that affect the resolution of image fiber are the diameter and arrangement manner of single optical fiber. The thinner the single fiber is, the better resolution the image fiber possesses. The hexagon array can get higher resolution than the square array in fiber bundle arrangement.

In addition, the fiber material, and the bundle cross-section area will also affect the quality of the image; the attenuation of plastic fiber is much higher than that of compound glass and silica. So, when choosing an image fiber bundle, we have to consider its numerical aperture, attenuation, resolution, material, and the diameter of the single fiber, length of the bundle and so on as a whole.

The image fiber bundles adopted in our system are made from compound glass. They are easier to be bent than the silica, and their attenuation is much smaller than the plastic. They can transmit the light wavelengths from 380 nm to 1300 nm. Their numerical aperture, attenuation and resolution are 0.55, 300~600 db/km and 36LP/mm, respectively.

### *3.2 Image processing*

Because lights cannot pass through the clad of the single fiber, many hexagonal grids appeared in the captured image (transmitted by an image fiber bundle). These grids have a great effect on the subsequent work, such as image processing, phase wrapping, 3D coordinate calculation and so on. How to reduce the grids efficiently is, therefore, crucial to the whole system. Generally speaking, two methods can be adopted for this problem. One is to select a more fibers bundle while remaining the image size constant; the other one is to apply image-processing technique. This study selected the latter approach with image smoothing algorithm by median filter [14]. The grids could be successfully removed.

## 4. EXPERIMENT RESULTS

In our investigations, we used a 600×800 DLP to project sine wave patterns. The gray level and the number of lines could be computer controlled. A compound glass image fiber bundle with 80,000 pixels was used to transmit the projected image.

The diameter of single fiber is 15μm, NA is 0.55, spectrum range is 380~1300nm. All the optical systems were designed by telecentric lenses. The measurement range is 4.5mm (L) x 3.6mm (W) x 1mm(H). The optical resolution is 120 LP/mm. A small optical head was designed to include the fiber bundle end, Optical System 2, Optical System 3, and the CCD, as illustrated in Fig. 9. The reflection angle is 45°. The end dimension of the head is 24mmx55mm. Fig. 10 shows the experimental setup.

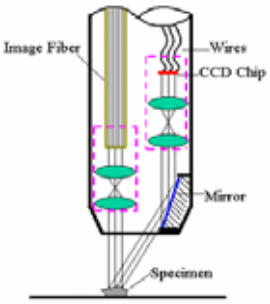


Fig. 9: The probe head design

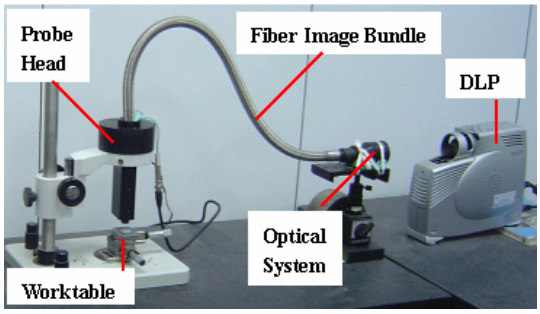


Fig. 10: The system setup

The system was calibrated by a gauge block of 1200μm to find the constant K of equation 7. With 7 times repeated tests, the averaged value was 1210μm with standard deviation 4.50μm.

In order to testify our system, we have inspected a V-groove with the size of 2.5mm×5mm by our system. Figs. 11(a) to (d) are the distorted images whose phases are 0º, 90º, 180º, and 270º respectively. Four-step phase shifting arithmetic was used to reconstruct the 3-D contour. Fig. 11(e) and Fig. 11(f) are the wrapped and the reconstructed 3-D contour.

The second case study was to measure a character of a Chinese one dime coin. The character size is about 4mmx3mm in surface area and 0.3mm in height, as shown in Fig. 12.

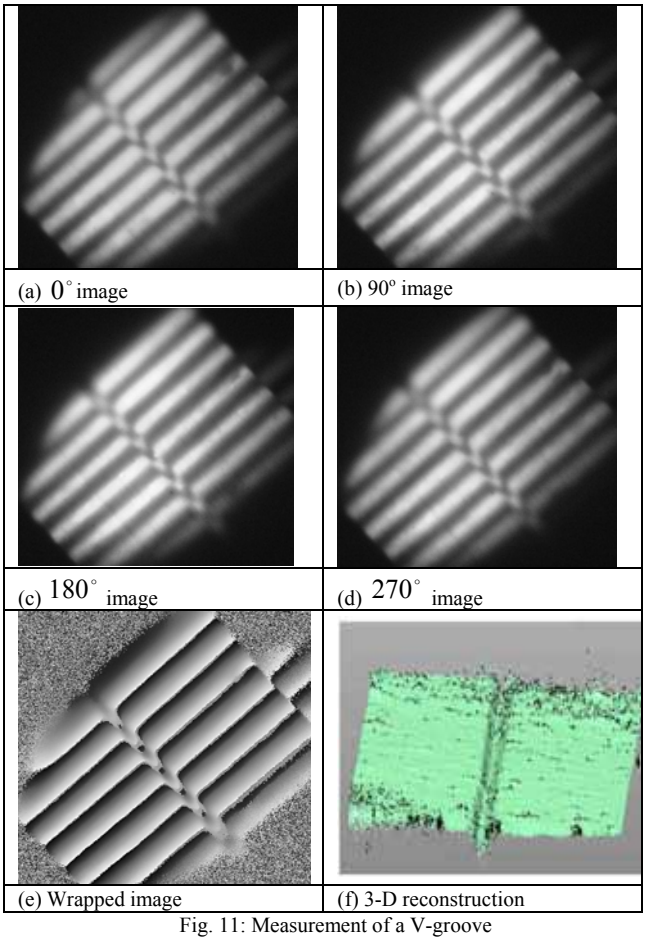

(a) $0^\circ$ image | (b) 90º image

(c) $180^\circ$ image | (d) $270^\circ$ image

(e) Wrapped image | (f) 3-D reconstruction

Fig. 11: Measurement of a V-groove

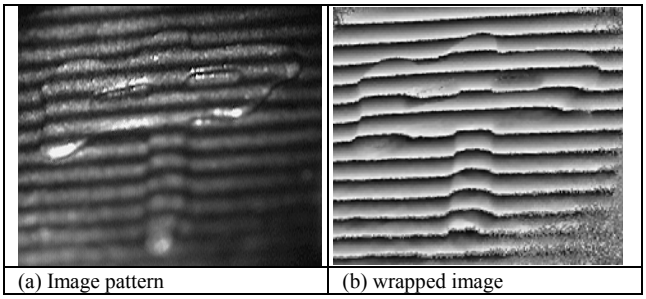

(a) Image pattern | (b) wrapped image

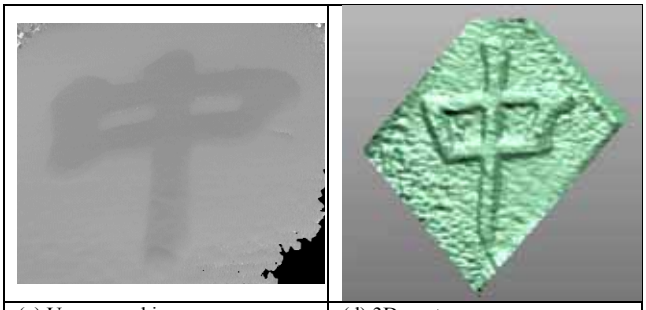

(c) Unwrapped image | (d) 3D contour

Fig. 12: Measured results of a character of a Chinese one dime coin

## 5. Concluding Remarks

A novel digital stereomicroscope system based on the fiber image technique is presented in this paper. Such a system overcomes the disadvantages of common stereomicroscopes in terms of extendable length and flexible orientation. It also realizes the concept of "adapt the instrument to the object". For any localized tiny portion of a large object, this system can easily move the optical head to the required position and take its 3D profile measurement. The feasibility of the system has been testified by the experiments.

Acknowledgement

The work reported forms part of a research program funded by the Tjing Ling Industrial Research Institute of National Taiwan University and the National Natural Science Foundation of China (50420120134).

## 6. References

[1]. Windecker, R., Fleischer, M., and Tiziani, H.J., "Three-dimensional topometry with stereomicroscopes," Opt. Eng. 36(12) 3372-3377, 1997.

[2]. Wu, S. D. and Lu, G. W., "Optical Phase Shift Triangulation Technique (PST) for Noncontact Surface Profiling," US Patent No. 6040910, 2000.

[3]. Zhang, C. P., Huang, P. S., and Chiang, F. P., "High-Speed Phase Shifting Profilometry," Proc. SPIE Vol. 4189, 122-128, 2001.

[4]. Song, H. M., "Development of a stereomicroscope," Master Thesis, National Taiwan University, 2004.

[5]. Bitte, F. and Dussler, G., "3D micro-inspection goes DMD," Optics and Lasers in Engineering Vol. 36, 155-167, 2001.

[6]. Younse, J. M., "Mirrors on a chip," IEEE Spectrum, 27-31, Nov.1993.

[7]. Creath, K., "Phase-measurement interferometry techniques," J. of Progress in Optics, 1988, 16: 351-393.

[8]. Macy, W. W., "Two-dimensional fringe-pattern analysis," J. of Applied Optics, 1983, 22: 3898 to 3901.

[9]. Huntley, J. M., "Noise-immune phase unwrapping algorithm," J. of Applied Optics, 1989, 28: 3268-3270.

[10]. Goldstein, R. M., Zebker, H. A., and Werner, C. L., "Satellite radar interferometry: two-dimensional phase unwrapping," J. of Radio Science, 1988, 23: 713-720.

[11]. http://www.edmundoptics.com/techsupport/

[12]. Rohr, S. and Kucera, J., "Optical Recording System Based on a Fiber Optic Image Conduit: Assessment of Microscopic Activation Patterns in Cardiac Tissue," Biophysics Journal, 1998, 75: 1062-1075.

[13]. http://floti.bell.ac.uk/MathsPhysics/fibre.htm

[14]. Gonzalez, R. C. and Wintz, P., "Digital Image Processing," Addison-Wesley Publishing Company, Inc., 1977.